Atomic-Scale Observations of Two-Dimensional Re Segregation at an Internal Interface in W(Re)

J. G. Hu and D. N. Seidman
Materials Science and Engineering Department, Northwestern University, Evanston, Illinois 60208
(Received 29 June 1990)

Equilibrium Re segregation is studied at a grain boundary in a single-phase W–25-at.%-Re alloy employing atom-probe field-ion microscopy. The grain-boundary concentration is measured, *without* data deconvolution, to be 73.8 ± 5.45 at.% Re at an interface plane. This is the first direct proof that segregation at a grain boundary can be purely two dimensional, and that it can occur at a so-called low-energy interface.

PACS numbers: 61.70.Ng, 02.50.+s, 61.16.Fk, 64.75.+g

The existence of two-dimensional monolayer gas adsorption at solid/gas interfaces[1] or two-dimensional monolayer solute-atom segregation at solid/vacuum interfaces[2] is now established both theoretically and experimentally. By analogy with the results on solid/gas or solid/vacuum interfaces it has been often asserted that equilibrium solute-atom segregation at solid/solid interfaces can be purely two dimensional and confined to a single monolayer. No comparable direct and unambiguous experimental evidence exists, however, for solid/solid interfaces,[3,4] and, furthermore, the quantitative relationship between grain-boundary (GB) structure and segregation under equilibrium thermodynamic conditions is lacking.[4]

Energy-dispersive x-ray and electron energy-loss spectroscopies in analytical electron microscopes (AEM's) have been employed to study GB segregation.[5,6] These spectroscopies require, however, assumptions to deconvolve the spatial distribution of segregants at an internal interface from the measured signals, even though atomic concentrations corresponding to fractions of a monolayer can be detected.[5,6] The spatial resolution of an AEM is limited by the geometric diameter of the electron beam plus the concomitant electron scattering that must occur. Therefore, the "composition of a monolayer" is often deconvolved subject to the assumption that segregation occurs in a monolayer.

Atom-probe field-ion microscopy (APFIM) can determine the chemical identity of a single preselected atom,[7] and it has been applied recently to the study of the chemical composition of internal interfaces.[8–13] To determine a segregation profile perpendicular to an internal interface requires the use of the geometry exhibited in Fig. 1; in this arrangement the spatial resolution is equal to the interplanar spacing of the planes parallel to the plane of the GB, and it is < 0.1 nm for a high-indexed plane. It is emphasized that this geometry does *not* require any deconvolution of the data and it measures directly the width of a concentration profile.

We present a combined transmission-electron-microscope (TEM), APFIM study of Re segregation at a GB in a single-phase W–25-at.%-Re alloy. The results demonstrate that Re segregation is localized in a *single* plane and is, therefore, two dimensional. This is the first *unequivocal* demonstration of this phenomenon at an internal interface, with a known crystallography, by any technique.

A W–25-at.%-Re wire (127-μm diam) was annealed at 1913 K for 5 h in flowing argon gas to induce Re segregation to GB's. This annealing time produces a root-mean-square diffusion distance of > 20 nm for the Re atoms; this was done to achieve, at the very least, local thermodynamic equilibrium of the Re atoms with GB's. At 1913 K a 25-at.%-Re alloy is a single-phase primary solid solution;[14] this is corroborated by the absence of precipitates in the grains examined by the TEM or APFIM techniques. Next the specimen was electropolished and electroetched to a sharply pointed tip (≈ 15-nm radius) that was suitable for TEM or APFIM observations.[11,13,15,16] After electropolishing, the specimen was mounted in a modified double-tilt stage[16] of a

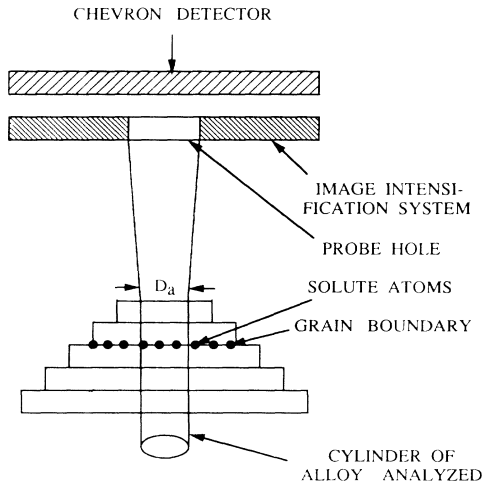

FIG. 1. The geometry employed for analyzing a GB, with its plane parallel to the plane of the probe hole (D_a). The solute profile perpendicular to the GB interface is determined with a spatial resolution equal to the interplanar spacing of the region analyzed. The diagram is not to scale.

200-kV TEM, and a GB located. The GB geometry was determined by TEM before the specimen was systematically backpolished to move the selected GB into the volume of the tip.[9,13,15,16]

Figure 2(a) exhibits a TEM micrograph of the FIM tip containing the GB; N.B., the interface plane is almost perpendicular to the [110] axis of the tip. By rotating the FIM specimen it was possible to orient the interface plane of the GB so that it was parallel to the plane of the chevron detector employed to detect the pulsed field-evaporated ions. An FIM image of the *same* GB is shown in Fig. 2(b). The black arrowheads on the periphery of the micrograph indicate its intersection with the surface of the FIM tip; the trace of the intersection of the GB with the approximately hemispherical tip is almost a perfect circle. The rotation angle (θ) of grain 1 (G1) with respect to grain 2 (G2) is $\theta = 88.7°$ about the rotation vector $\mathbf{c} = [0.700.720.01]$. The nearest coincident site lattice (CSL) is $\Sigma = 17$ ([110]/86.63°), and the disorientation is [221]/61.93°.[17-19] The $\mathbf{n}$'s to this GB, in the coordinates of G1 and G2, are $\mathbf{n}_1 = [-0.79\ -0.600.13]_1$ and $\mathbf{n}_2 = [0.620.77\ -0.12]_2$. The vectors $\mathbf{n}_1$ and $\mathbf{n}_2$ are 2.6° and 1.0° from the $[-6\ -51]$ and $[56\ -1]$ directions, respectively; the $\langle 651 \rangle$ direction is the nearest rational direction to $\mathbf{n}$. The angle between $\mathbf{c}$ and $\mathbf{n}$ is $\approx 10.5°$ and therefore this GB is almost a pure twist boundary with a small tilt component. The results of this crystallographic analysis were verified from an analysis of the FIM image; it is noted, however, that the five macroscopic degrees of freedom of the interface —i.e., the $\mathbf{c}/\theta$ pair—were determined by TEM.

The misorientation of this GB deviates from the nearest CSL orientation by $\Delta\theta \approx 2.5°$, as calculated from the measured deviation matrix. The maximum allowable value of $\Delta\theta_c$, within which a CSL relationship is maintained by the introduction of secondary grain-boundary dislocations, is given by $\Delta\theta_c \approx 15°(\Sigma)^{-1/2}$.[20] For $\Sigma = 17$ the value of $\Delta\theta_c$ is 3.64°, and since $\Delta\theta$ is $< \Delta\theta_c$ this GB can be described by the above CSL description, and therefore it is a so-called special boundary.

An APFIM analysis of this *same* GB was executed using the geometry of Fig. 1. The cylindrical volume of the metal alloy analyzed was perpendicular to the plane of the GB, and therefore a series of *individual* $\approx (651)$ planes parallel to the interface was analyzed chemically. The number of atoms covered by the probe hole for this analysis was 65; the APFIM time-of-flight data were collected at a specimen temperature of 30 K using a pulse fraction (f)—the ratio of the pulse voltage to the dc voltage—of $f = 0.15$, and a background vacuum of $< 10^{-8}$ Pa. The detection efficiency was maintained at a low value by increasing the steady-state evaporation voltage in 15-V dc increments every 1200 field-evaporation pulses if no event was detected; if an event was detected then the code was reset automatically to request an additional 1200 pulses. Figure 3 is an integral profile of the cumulative number of Re atoms versus the cumulative number of W plus Re atoms; therefore the local slope is directly equal to the average Re concentration of either the matrix or the GB. This figure demonstrates that the concentration changes from $\langle C_{Re} \rangle = 24.8 \pm 1.79$ at.% Re (Ref. 21) to $\langle C_{Re}^{gb} \rangle = 73.8 \pm 5.45$ at.% Re and then back to $\langle C_{Re} \rangle = 25.4 \pm 1.17$ at.% Re, as the GB is traversed. The evaporation rate for the matrix was 6×10^{-3} atoms pulse^{-1}, while for the region of the GB it was 3×10^{-3} atoms pulse^{-1}. Thus the evaporation rate for the GB region was *lower* than for the matrix and therefore it was dissected more slowly and more carefully than the matrix. In fact, most of the events detected from the GB were single-channel events. A total of 65 W and Re atoms are in the region corresponding to

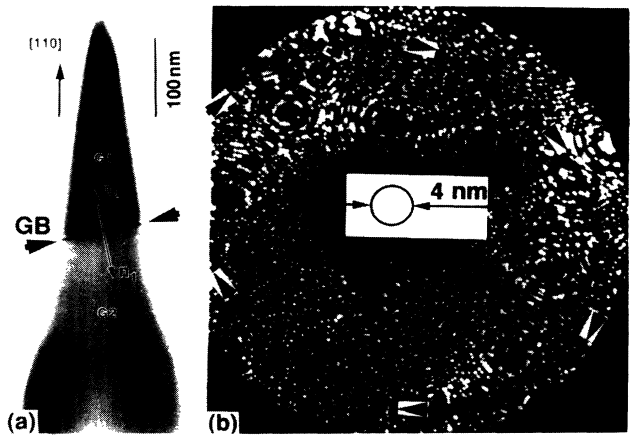

FIG. 2. (a) A TEM micrograph of the analyzed GB in the FIM specimen. (b) An FIM micrograph of the *same* GB. The black arrowheads indicate the intersection of the GB with the approximately hemispherical FIM tip.

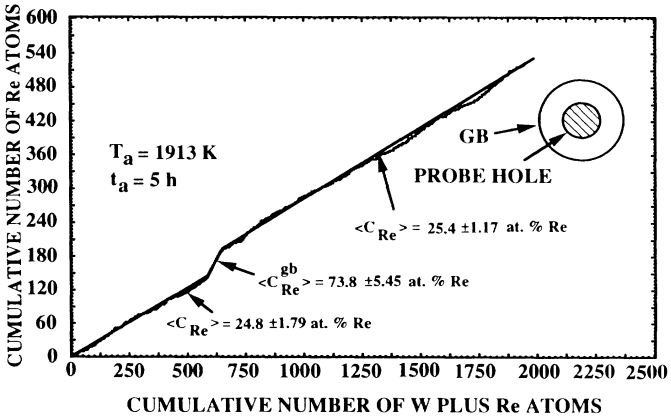

FIG. 3. An integral profile of the cumulative number of Re atoms versus the cumulative number of W plus Re atoms for the matrix and the GB seen in Fig. 2; the data were recorded at a specimen temperature of 30 K.

73.8 ± 5.45 at.% Re. Figure 4 is a plot of the Re concentration in individual planes versus depth employing 65 atoms to calculate the Re concentration for each plane in the matrix; each plane is numbered on the lower abscissa axis; and the top abscissa axis is the cumulative number of W plus Re atoms. The solute concentration is observed to increase from $\langle C_{Re} \rangle = 29.2 \pm 5.64$ to 73.8 ± 5.45 at.% Re in *one* interplanar spacing— ≈ 0.04 nm—and the to decrease to 23.1 ± 5.23 at.% Re in *one* interplanar spacing; N.B., the planes numbered 9, 10, and 11. The value of $\langle C_{Re} \rangle$ is 25.2 ± 0.98 at.% Re averaged over 29 planes—excluding the interface plane. This result demonstrates that for this alloy and this GB the Re segregation is localized at *one* plane, and for the planes that immediately adjoin this interface plane the concentration is $\approx \langle C_{Re} \rangle$. This implies an average segregation enhancement factor S_{ave} of 2.9, where S_{ave} is the ratio of the average solute concentration at a GB to $\langle C_{Re} \rangle$. The data represent direct and unambiguous evidence for two-dimensional segregation; it is emphasized that for the geometry used *no* corrections of the experimental data are required. The concentration values are absolute, as they are determined on the basis of counting *individual* atomic events in *individual* atomic planes.

The data in Fig. 4 show that the Re segregation is purely two dimensional at a $\Sigma \approx 17$ [$\approx (651)$] interface; the (651) interplanar spacing is ≈ 0.04 nm. The concentration in this plane corresponds to $\approx \frac{3}{4}$ of a monolayer of Re. These results demonstrate several important physical points. First, significant segregation of Re occurs even though the solid-solubility limit of Re in W is appreciable at 1913 K; thus, limited solid solubility of the solute is *not* a necessary condition for GB segregation.[22] Second, the observation of Re segregation at a so-called special GB—i.e., a small Σ value—is counter to the intuitive idea that segregation should be smaller at special GB's than at general boundaries, because the atomic fit is better at the special GB's—i.e., they are lower-energy interfaces.[4] There are still no general principles that relate the interfacial free energy of a GB to the geometry [Σ and (hkl) values] of an interface.[23] Furthermore, the depths of the energy cusps of special GB's relative to the energy of general GB's are unknown. Thus special GB's may have an energy less than the general GB's, but these energies can be significantly greater than the energy of a small-angle ($< 15°$) GB. Furthermore, we have employed Monte Carlo computer simulations to study the structural and temperature dependence of Au segregation to [001] twist boundaries—between $\theta = 0°$ and 45° in a Pt-1-at.%-Au alloy between 850 and 1900 K.[24] The results of simulations show that the value of S_{ave} increases linearly to $\theta \approx 35°$ and is independent of θ between 35° and 45°. The simulations furthermore demonstrate that Au segregation occurs primarily substitutionally at the cores of the primary GB dislocations, and that S_{ave} saturates when the cores overlap strongly. Thus we can interpret the Re segregation as occurring at the cores of the dislocations associated with the $\Sigma \approx 17$ [$\approx (651)$] GB studied. Third, the GB concentration corresponds to the composition of the χ phase (≈ 75 at.% Re) on the bulk phase diagram.[14] Since the Re segregation is two dimensional it is possible that an ordered phase may form at the GB. A two-dimensional ordered phase implies that superlattice reflections should appear around the primary reflections from the matrix in a selected-area diffraction pattern of a GB; the intensity of a superlattice reflection is proportional to the square of the difference of the electron scattering factors—this is very small for W ($Z = 74$) and Re ($Z = 75$). These superlattice reflections may be detectable using a TEM with a bright field-emission electron source. Fourth, in contrast to the present results, solute segregation at an internal interface need not be purely two dimensional. For example, we have recently presented evidence for an oscillatory Ni profile at a $\Sigma \approx 5$ [$\approx (202)$] GB in a Pt-3-at.%-Ni alloy in a grain that consists of $(10\,\bar{6}\,8)$ planes; the latter are vicinal to the $(1\,\bar{1}\,1)$ planes.[25] In the other grain that adjoins the interface the Ni profile decreases monotonically to 3 at.% Ni. Thus, pure two-dimensional segregation can occur but it is not a universal mode for solute segregation at a GB. These results are readily understood by recalling that for a locally relaxed boundary $6+C$ state variables are required to specify the thermodynamic state of the system, where C is the number of chemical components.[26] For a binary alloy an eight-dimensional hyperspace is therefore involved, and each point in this hyperspace represents a thermodynamic state of a GB; the eight state variables are the five macroscopic degrees of freedom, tempera-

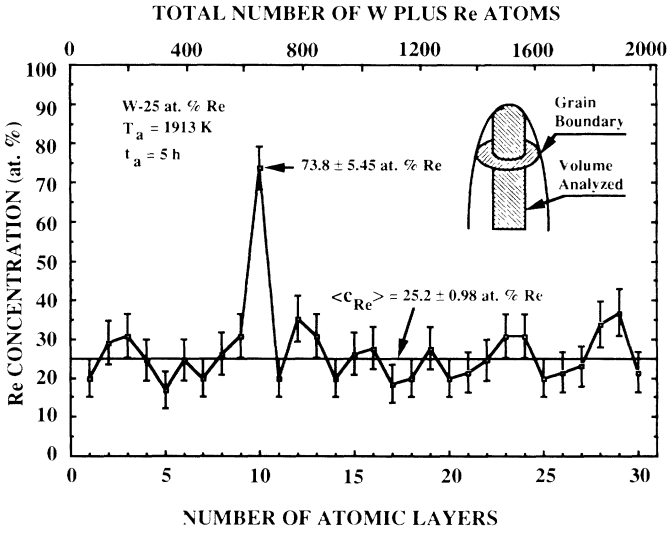

FIG. 4. The Re concentration profile perpendicular to the plane of the GB calculated from the data in Fig. 3. Each point corresponds to the Re concentration in a *single* plane; it increases from $\langle C_{Re} \rangle$ to 73.8 ± 5.45 at.% Re in one interplanar spacing— ≈ 0.04 nm—and then decreases to $\langle C_{Re} \rangle$ in one interplanar spacing.

ture, pressure, and bulk composition. Thus, it is thermodynamically possible for a particular boundary in a binary alloy to have an oscillatory solute profile, and a different type of boundary in a different binary alloy to have a simple two-dimensional solute profile. Fifth, in view of the above we do not think it is meaningful to think of solute segregation at GB's in terms of its Σ value and whether it is a special or general boundary. Instead it is more physically meaningful to specify the point in the hyperspace representing the thermodynamic state of the GB by the requisite GB state variables.

This research is supported by National Science Foundation Grant No. DMR-8819074. It utilized central facilities of the NSF-funded Materials Research Center. We thank Professor G. B. Olson for use of the VG APFIM, and Dr. F.-R. Chen, Dr. T. Kinkus, and Dr. D. Udler for useful discussions.

[1]A. Zangwill, *Physics at Surfaces* (Cambridge Univ. Press, New York, 1988), Chaps. 8 and 9.

[2]J. M. Blakely, J. Phys. (Paris), Colloq. **49**, C5-351 (1988).

[3]M. Guttmann, Metall. Trans. A **8**, 1383 (1977).

[4]R. W. Balluffi, in *Interfacial Segregation* (American Society for Metals, Metals Park, OH, 1979), pp. 193–237.

[5]J. R. Michael and D. B. Williams, Metall. Trans. A **15**, 99 (1984); M. Hellsing, Metall. Trans. A **16**, 686 (1985); D. B. Williams and A. D. Romig, Jr., Ultramicroscopy **30**, 38 (1989).

[6]C. Colliex, J. L. Maurice, and D. Ugarte, Ultramicroscopy **29**, 31 (1989).

[7]R. Wagner, *Field-Ion Microscopy in Materials Science* (Springer-Verlag, Berlin, 1982); D. N. Seidman, in *Encyclopedia of Materials Science & Engineering,* edited by M. B. Bever (Pergamon, Oxford, 1986), pp. 1741–1744; T. Sakurai, A. Sakai, and H. W. Pickering, *Atom-Probe Field Ion Microscopy and Its Applications* (Academic, Boston, MA, 1989); M. K. Miller and G. D. W. Smith, *Atom Probe Microanalysis* (Materials Research Society, Pittsburgh, PA, 1989).

[8]R. Herschitz and D. N. Seidman, Scripta Metall. **16**, 849 (1982); Acta Metall. **33**, 1547 (1985); **33**, 1565 (1985).

[9]L. Karlsson and Nordén, Acta Metall. **36**, 13 (1988).

[10]D. D. Sieloff, S. S. Brenner, and M. G. Burke, Mat. Res. Soc. Symp. Proc. **81**, 87 (1989); P. P. Camus, I. Baker, J. A. Horton, and M. K. Miller, J. Phys. (Paris), Colloq. **49**, C6-329 (1988).

[11]J. G. Hu, S.-M. Kuo, A. Seki, B. W. Krakauer, and D. N. Seidman, Scripta Metall. **23**, 2013 (1989).

[12]D. N. Seidman, Mat. Res. Soc. Symp. Proc. **138**, 315 (1989); **139**, 25 (1989).

[13]L. V. Alvensleben and P. Haasen, Mat. Res. Soc. Symp. Proc. **138**, 479 (1989).

[14]J. M. Dickinson and L. S. Richardson, Trans. Amer. Soc. Met. **51**, 758 (1959); R. K. Williams, F. W. Wiffen, J. Bentley, and J. O. Stiegler, Metall. Trans. A **14**, 655 (1983).

[15]J. E. Fasth, B. Loberg, and H. Nordén, J. Sci. Instrum. **44**, 1044 (1967); B. Loberg and H. Nordén, Ark. Fys. **39**, 383 (1969).

[16]B. W. Krakauer, J. B. Hu, S.-M. Kuo, R. Mallick, A. Seki, D. N. Seidman, J. Baker, and R. Loyd, Rev. Sci. Instrum. (to be published).

[17]F.-R. Chen and A. H. King, J. Electron. Microsc. Tech. **6**, 55 (1987).

[18]W. Bollmann, *Crystal Lattices, Interfaces, Matrices* (Imprimerie des Bergues, Geneva, 1982), pp. 336–338.

[19]The GB misorientation is given by a $\mathbf{c}/\theta$ pair. For cubic symmetry there are 1152 equivalent $\mathbf{c}/\theta$ pair descriptions of the same GB. The disorientation is for the smallest θ with the $\mathbf{c}$ vector pointing in the standard stereographic triangle (Ref. 18). The wire texture implies that the GB's can be described as a rotation about the [110] axis although it is *not* necessarily the disorientation vector.

[20]D. G. Brandon, Acta Metall. **14**, 1479 (1966).

[21]The $\pm$ uncertainty is the standard error of the mean and is equal to $(N_{\mathrm{Re}}N_{\mathrm{W}})^{1/2}(N_{\mathrm{Re}}+N_{\mathrm{W}})^{-3/2}$ where N is the number of Re or W atoms; C. Mack, *Essentials of Statistics for Scientists and Technologists* (Plenum, New York, 1967), pp. 34–35.

[22]E. D. Hondros and M. P. Seah, in *Physical Metallurgy,* edited by R. W. Cahn and P. Haasen (Elsevier, New York, 1983), Vol. 1, Chap. 13.

[23]A. P. Sutton and R. W. Balluffi, Acta Metall. **35**, 2177 (1987).

[24]A. Seki, D. N. Seidman, Y. Oh, and S. M. Foiles (to be published).

[25]S. M. Kuo, A. Seki, Y. Oh, and D. N. Seidman, Phys. Rev. Lett. **65**, 199 (1990).

[26]J. W. Cahn, J. Phys. (Paris), Colloq. **43**, C6-199 (1982).

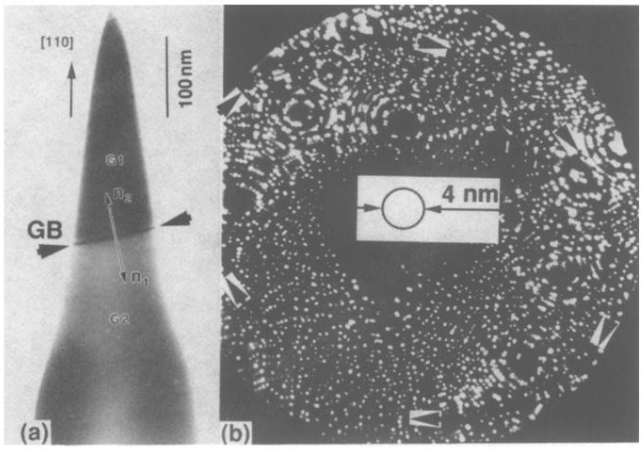

FIG. 2. (a) A TEM micrograph of the analyzed GB in the FIM specimen. (b) An FIM micrograph of the *same* GB. The black arrowheads indicate the intersection of the GB with the approximately hemispherical FIM tip.